

## Cobalt growth on Cu(111) in the presence of indium surfactant

H. Wider, V. Gimple, W. Evenson, G. Schatz, J. Jaworski, and M. Marszaek

Citation: *Journal of Applied Physics* **95**, 5837 (2004); doi: 10.1063/1.1710723

View online: <http://dx.doi.org/10.1063/1.1710723>

View Table of Contents: <http://scitation.aip.org/content/aip/journal/jap/95/10?ver=pdfcov>

Published by the [AIP Publishing](#)

---

### Articles you may be interested in

[Oxygen surfactant-assisted growth and dewetting of Co films on O-3×3/W\(111\)](#)

*J. Appl. Phys.* **114**, 203907 (2013); 10.1063/1.4833570

[Ag as a surfactant for Co/MgO\(111\)-\(3 × 3\)R 30°](#)

*J. Vac. Sci. Technol. A* **31**, 061518 (2013); 10.1116/1.4826704

[Characterization of ALD copper thin films on palladium seed layers](#)

*J. Vac. Sci. Technol. A* **27**, 660 (2009); 10.1116/1.3143663

[Enhancement in layer-by-layer growth in heteroepitaxial growth of Co on Au\(111\) surface by Bi surfactant](#)

*J. Appl. Phys.* **100**, 113532 (2006); 10.1063/1.2400106

[Bi: Perfect surfactant for Ge growth on Si\(111\)?](#)

*Appl. Phys. Lett.* **74**, 1391 (1999); 10.1063/1.123560

---



## Re-register for Table of Content Alerts

Create a profile.



Sign up today!



## Cobalt growth on Cu(111) in the presence of indium surfactant

H. Wider, V. Gimple, W. Evenson,<sup>a)</sup> and G. Schatz<sup>b)</sup>

*Department of Physics, University of Konstanz, D-78457 Konstanz, Germany*

J. Jaworski and M. Marszałek

*The H. Niewodniczański Institute of Nuclear Physics PAN, Kraków, Poland*

(Received 14 November 2003; accepted 26 February 2004)

The effect of a pre-deposited ultrathin film of indium on the deposition of cobalt on Cu(111) has been studied by an *in situ* combination of medium energy electron diffraction, scanning tunneling microscopy, and Auger electron spectroscopy. Pre-deposited indium allows cobalt to deposit in layer-by-layer growth, in contrast to the three-dimensional growth observed without the indium surfactant. The surfactant effect is connected to the surface alloys, Cu<sub>2</sub>In and Cu<sub>3</sub>In, that form upon indium pre-deposition. Initial cobalt nucleation processes and indium segregation during cobalt deposition are also discussed. © 2004 American Institute of Physics. [DOI: 10.1063/1.1710723]

### I. INTRODUCTION

Ultrathin metallic films and multilayer systems made up of thin metallic layers are of significant technical and fundamental interest. This is especially true for layered systems of magnetic materials. Studies of multilayers of 3*d*-transition metals have resulted in the discovery of new physical phenomena, including magnetic interlayer coupling<sup>1–3</sup> and giant magnetoresistance (GMR),<sup>4</sup> phenomena that have already provided technology for new sensor elements.<sup>5</sup> Cobalt/copper layered systems have shown the largest potential for such technological applications, so that in sputter-deposited multilayers, preferentially exhibiting (111) orientation, GMR effects have been obtained of up to 65% at ambient temperature.<sup>6–8</sup>

The GMR properties of these multilayers depend strongly on the quality of the Co–Cu layers, because interface quality strongly affects the oscillatory exchange coupling that gives rise to GMR behavior.<sup>9</sup> In systems with one or more spatial dimensions in the range of nanometers, confinement in the small dimension plays a crucial role in interlayer magnetic coupling. Therefore, the physical characteristics are often drastically modified by broken symmetry at surfaces and interfaces. Whereas, if the film layers and interfaces are of sufficient quality, one can tune the GMR and magnetic properties of these devices.<sup>10–16</sup>

Some reasonable approximation to layer-by-layer growth is required to manufacture films of high structural quality with smooth boundary surfaces. Unfortunately, this growth mode often does not automatically result from deposition processes for a given material combination of substrate and adsorbate, and it often cannot be achieved simply by variation of the controllable deposition parameters. For example, substantial interdiffusion at the interface frequently results

from increased substrate temperature rather than layer-by-layer growth.

The presence of a surfactant can help solve these problems by assisting layer-by-layer growth. A surfactant is an additional species laid down on the substrate before deposition of the adsorbate. The surfactant species modifies the structural and physical characteristics of the layers and their boundary surfaces.<sup>17</sup> In a simple picture, the surfactant plays the role of a growth catalyst and usually improves the growth of the deposited film by making atomically smooth two-dimensional (2D) layer-by-layer growth more energetically favorable than the rough, three-dimensional (3D) island growth that is favored without the surfactant. Ideally, the surfactant species should constantly segregate to the surface by site exchange processes and be available for the growth of the next atomic layer, thus incorporating only a minimal amount of this additional material into the growing film.

Inspired by successes with metallic surfactant species such as indium (In), antimony (Sb), and arsenic (As) in semiconductor epitaxy, several groups in the early 1990s began to examine the influence of these elements on the growth of metallic thin film systems. The first system studied was Ag/Ag(111) with antimony as surfactant, by van der Vegt *et al.* using *in situ* x-ray diffraction.<sup>18</sup> Later scanning tunneling microscopy (STM) investigations of this system<sup>19</sup> also showed modified nucleation behavior, leading to irregular but flat islands in the presence of antimony, in contrast to 3D islands with smooth edges without antimony. These results suggest that antimony lowers the surface mobility of Ag adatoms, as well as diffusion along island edges. Further STM investigations of this system<sup>20</sup> showed that antimony prefers substitutional lattice sites in the highest silver layer and stays in the topmost layer by site exchange processes with silver adatoms, either inside one of the islands or at an edge.

Surfactant effects of indium in metal–metal adsorbate–substrate systems have also been shown in earlier work.<sup>21–23</sup> The present work shows that indium plays such a role in the Co–Cu(111) system. In addition, the details of indium's action and segregation in this system were studied. Because indium atoms are much larger than either cobalt or copper

<sup>a)</sup>Permanent address: School of Science & Health, Utah Valley State College, Orem, UT 84058.

<sup>b)</sup>Author to whom correspondence should be addressed; electronic mail: guenter.schatz@uni-konstanz.de

(metallic radii:  $r_{\text{In}}=0.1663$  nm,  $r_{\text{Cu}}=0.1278$  nm,  $r_{\text{Co}}=0.1252$  nm),<sup>24</sup> the specifics of indium's surfactant activity in the deposition of cobalt on copper are interesting in themselves: how do dissolution and segregation take place when cobalt is deposited on the close-packed Cu(111) surface with a preexisting thin film of indium consisting of such large atoms?

We have found previously that indium forms ordered surface alloys on Cu(111) that are unknown in the bulk.<sup>25</sup> As discussed below, this behavior helps clarify the interaction of indium with cobalt and copper in cobalt deposition on Cu(111).

Cobalt layer growth on Cu(111) was investigated in the present work as a function of an intermediate indium layer by an *in situ* combination of medium energy electron diffraction (MEED), scanning tunneling microscopy (STM), and Auger electron spectroscopy (AES). The morphology of growth and the nucleation behavior were examined.

## II. EXPERIMENTAL DETAILS

Sample preparation and characterization were done in an ultrahigh-vacuum system at pressures below  $10^{-8}$  Pa. Copper single crystals were prepared from a (111)-oriented rod that was polished mechanically and electrochemically. The Cu(111) surface was cleaned in ultrahigh vacuum by alternate cycles of argon ion sputtering (argon energy, 250–760 eV) and annealing at 600 °C for times ranging from 5 min to 1 h per cycle.

Indium films were deposited at rates between 0.05 and 0.5 ML/min by thermal evaporation at a working pressure in the range of  $10^{-8}$  Pa. Indium film thickness was controlled during evaporation with a quartz thickness monitor, and ML-In were defined to be equivalent ML of pure indium layers with the bulk indium lattice constant. During deposition the sample was kept at room temperature.

Cobalt films were deposited by electron gun evaporation, also at a working pressure of about  $10^{-8}$  Pa, with voltage about 800 V, filament current about 2 A, and flux current 105  $\mu$ A. This gives a deposition rate of about 0.6 ML/min. Cobalt film thickness was estimated from the deposition time and from monolayer MEED oscillations. Similar to indium, ML-Co were defined to be equivalent ML of pure cobalt layers with the bulk cobalt lattice constant. The sample was kept at room temperature during cobalt deposition.

At each step the sample surface was checked *in situ* by AES and never showed residual gas contamination greater than 0.01 ML. Peak-to-peak AES intensities were measured during deposition of cobalt for the 716 eV (*LMM*) Co line, the 920 eV (*LMM*) Cu line, and the 404 eV (*MNN*) In line.

Film growth was monitored *in situ* by MEED (2.7 keV). MEED intensity measurements were taken from windows positioned at various points on specular reflections. Relative lattice constant changes were measured by accurate line scans showing spot separations during deposition of indium or cobalt.

After deposition, the sample surface was analyzed with a commercial STM from RHK, Inc., that operates at variable temperatures from 100 to 500 K.

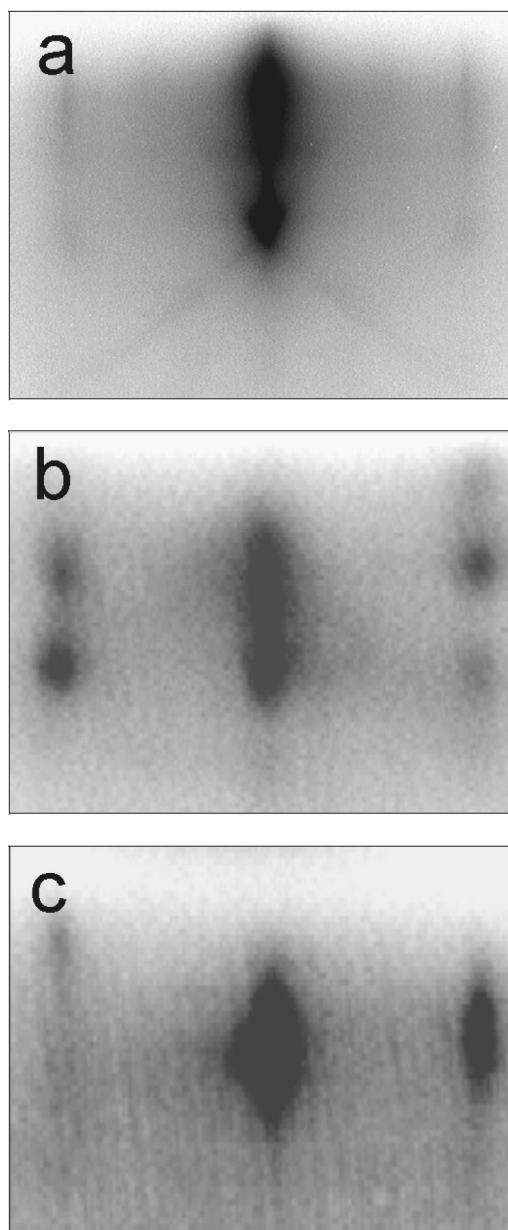


FIG. 1. Typical MEED specular reflection spots for (a) clean Cu(111) surface, (b) 6 ML Co on Cu(111), and (c) 6.2 ML-Co on Cu(111) with 0.5 ML pre-deposited In. The reflection spots were recorded at the  $\langle 1\ 1\ -2 \rangle$  azimuthal angle.

## III. RESULTS

The deposition of cobalt on Cu(111) results in three-dimensional island growth, as observed previously<sup>26,27</sup> and consistent with our MEED measurements. The MEED specular beam intensity was observed during cobalt deposition, both with and without pre-deposited indium. Typical MEED specular reflection spots are shown in Fig. 1 for a clean Cu(111) surface, Co on Cu(111), and Co on Cu(111) with pre-deposited In. Without indium, Fig. 1(b) shows that deposition of cobalt results in first-order spots characteristic of three-dimensional growth, rather than streaks, as would be characteristic of two-dimensional (i.e., layer) growth. The shift from streaks to spots occurs at about 3 ML-Co on the copper surface.

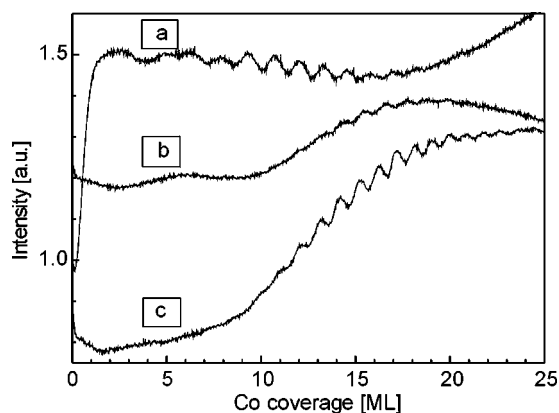


FIG. 2. MEED intensities at selected points in the reflection spots (where MEED oscillations were observed) for (a) 0.66 ML pre-deposited indium, (b) 1 ML pre-deposited indium, and (c) 3 ML pre-deposited indium.

Compare Fig. 1(b) with Fig. 1(c) to see the effect of indium pre-deposition: now for 6.2 ML-Co, with 0.5 ML-In, we again see streaks at the first-order positions, characteristic of two-dimensional structures.

We measured the evolution of the intensities at several points in the extended reflection spots simultaneously during cobalt evaporation. We looked especially for MEED oscillations, which are indicative of layer-by-layer growth. Other features of the MEED intensity patterns were also identified, where possible, as indicators of changes in growth modes. Figure 2 shows MEED intensities at selected points in the reflection spots (where MEED oscillations were observed) for three different indium pre-deposition coverages.

The relative change in the in-plane lattice constant due to cobalt deposition, with and without indium incorporation, is shown in Fig. 3, as measured by the separation of the MEED spots during cobalt deposition. The surface lattice constant decreased by about 1.6% relative to the pure copper surface lattice constant with full cobalt coverage [Fig. 3(a)].

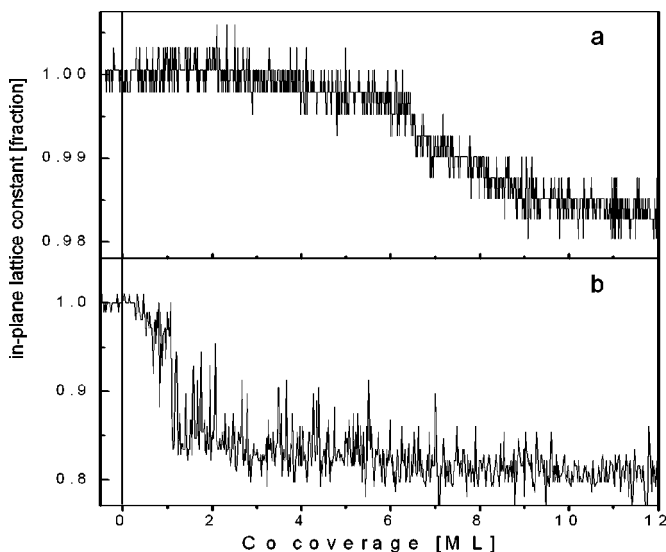


FIG. 3. Relative in-plane lattice constant as a function of cobalt coverage: (a) without pre-deposited indium and (b) with nominal 1 ML pre-deposited indium.

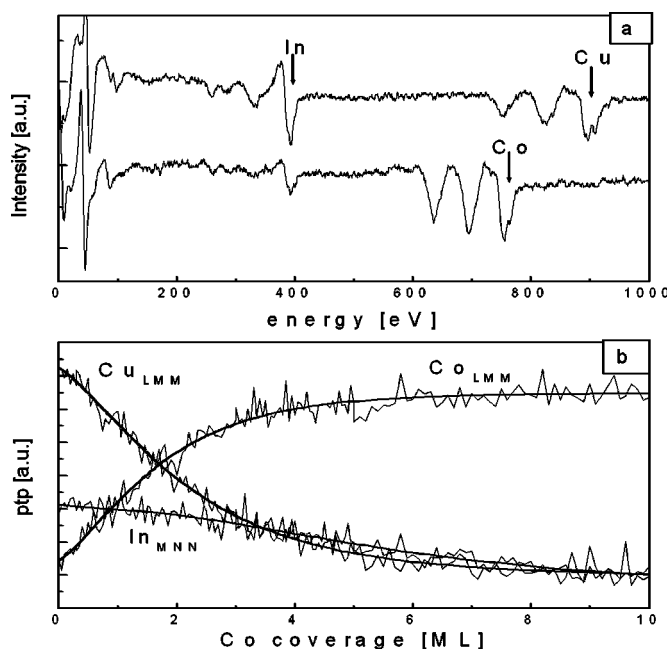


FIG. 4. Auger spectra. (a) Spectral derivative intensity with 0.5 ML pre-deposited indium before (upper curve) and after (lower curve) deposition of 12 ML-Co. (b) Peak-to-peak intensities measured during deposition of cobalt on a sample with 0.1 ML pre-deposited indium for cobalt 716 eV, indium 404 eV, and copper 920 eV Auger electrons.

With the pre-deposition of about 1 ML indium, which first expands the copper surface lattice,<sup>25</sup> deposition of cobalt caused the surface lattice constant to decrease much more quickly by about 16% [Fig. 3(b)].

AES measurements are shown in Fig. 4 as a function of cobalt coverage with pre-deposited indium. Figure 4(a) shows two spectra with 0.5 ML pre-deposited indium, before and after deposition of 12 ML-Co. This figure shows that indium, but not copper, is still visible even after depositing cobalt to a coverage of 12 ML. Peak-to-peak intensity of 716 eV cobalt Auger electrons, measured during the deposition of cobalt on a sample with 0.1 ML pre-deposited indium [Fig. 4(b)], increased with cobalt coverage up to about 4 ML-Co. Indium 404 eV Auger electron intensity decreased slowly after the first few monolayers of cobalt deposition. This decrease in the indium line was certainly not exponential, but approximately linear. The peak-to-peak intensity of the copper 920 eV line decreased approximately exponentially during cobalt deposition.

Figure 5 shows STM images of the surface development as cobalt is deposited, both with and without the presence of indium. Note that these STM images show microscopic local topography, while MEED and AES provide information on macroscopic structure on the scale of the beam size. Without pre-deposited indium, cobalt forms randomly positioned islands on the Cu(111) surface [Fig. 5(a)] that gradually fill up the surface but are irregular in height, even up to 2.5 ML-Co [Fig. 5(b)]. On the other hand, with 0.33 ML pre-deposited indium [Figs. 5(c) and 5(d)], cobalt again forms randomly positioned islands initially. However, these islands grow with

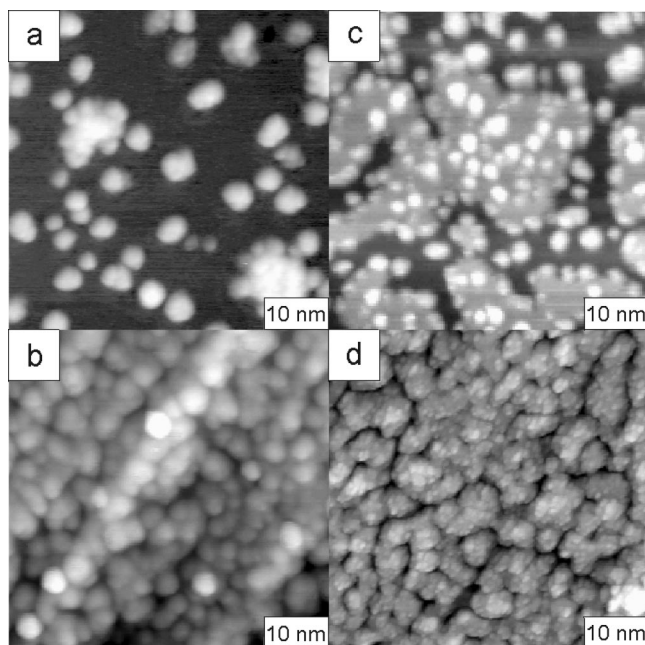


FIG. 5. STM images of surface development as cobalt is deposited, without pre-deposited indium (a), (b) and with 0.33 ML pre-deposited indium (c), (d). Cobalt coverages are (a) 0.1 ML, (b) 2.5 ML, (c) 0.25 ML, (d) 2.5 ML.

higher density and fill the surface more evenly, as can be seen quantitatively in the island size histograms discussed below.

#### IV. EFFECT OF In ON Co GROWTH

Pre-deposition of up to 0.5 ML-In results in the formation of a  $\text{Cu}_2\text{In}$  surface alloy. More than 0.5 ML-In pre-deposited leads to a  $\text{Cu}_3\text{In}$  alloy that assembles through multiple layers at the copper surface.<sup>25</sup> The presence of these alloys plays a crucial role in the growth of cobalt on Cu(111), as we discuss below.

Figure 3, showing the in-plane lattice constant during deposition of cobalt, leads to a simple picture of cobalt growth with and without indium pre-deposition. Without indium, the pure copper surface has an in-plane lattice constant of 0.2556 nm. The metallic radius of cobalt atoms is 0.1252 nm, which would give an in-plane lattice constant of 0.2504 nm, i.e., 98% of the pure copper case, consistent with the change of lattice constant seen by quantitative MEED analysis when the copper surface is fully covered by several monolayers of cobalt. Note that it takes at least 5 ML Co to achieve this full reduction of in-plane lattice constant, consistent with the observation that cobalt deposited on pure copper forms islands initially.

With pre-deposited indium, on the other hand, the mean in-plane lattice constant increases to 0.295 nm, i.e., 15% greater than pure copper.<sup>25</sup> Then when cobalt is deposited, the cobalt atoms apparently replace indium in the copper-indium alloy, reducing the mean in-plane lattice constant to 0.253 nm, now a decrease to 86% of the starting point, consistent with Fig. 3. The geometry of the MEED experiment is set up to sample the surface layer, allowing us to conclude that the lattice constant decrease takes place in the first

monolayer of cobalt, strongly supporting the suggestion that cobalt is simply replacing indium in the surface alloy.

The surfactant behavior of indium is thus viewed as follows: indium first forms a surface alloy with copper, in effect preparing the surface for cobalt, which exchanges sites with indium in the copper surface. Following the exchange, indium atoms are again at the top layer and again interact with incoming cobalt atoms in forming new nucleation centers. This process approximately repeats until deposition is complete. That it does not repeat exactly is seen from the gradual, approximately linear decrease in the indium AES intensity during cobalt deposition [Fig. 4(b)], showing that indium does get covered by cobalt, but not in its original position, which would produce an exponential AES intensity decrease.

One can consider whether the near linear indium AES intensity decrease could be caused by island (3D) growth of cobalt, partially covering the indium layer. That this is not so is seen from the MEED data in Figs. 1 and 2. Figure 1 shows a clear change from 3D growth to 2D (layer) growth with the pre-deposition of indium. Figure 2 shows oscillations due to changes in the cobalt surface roughness and indicative of layer-by-layer growth, again only with pre-deposited indium. Furthermore, the AES data show that copper is fully covered as cobalt is deposited since the copper Auger intensity decreases approximately exponentially, in clear contrast to the indium Auger intensity.

The AES data of Fig. 4(a) confirm the interpretation of Fig. 4(b) and the related discussion above by showing that indium can still be seen after 12 ML-Co has been deposited, while the copper signal has completely disappeared. At an incidence angle of  $77^\circ$  the 920 eV copper Auger electrons have an effective mean penetration depth of 0.38 nm, the 716 eV cobalt electrons 0.34 nm, and the 404 eV indium electrons 0.25 nm.<sup>25</sup> One monolayer of cobalt is 0.204 nm thick, so these correspond to 1–2 ML-Co, clearly indicating that indium has continued to migrate close to the surface during cobalt deposition.

Finally, the STM images shown in Fig. 5 illustrate the growth in the absence and presence of indium on a much finer spatial scale than MEED and AES data represent. Nevertheless, we see in Figs. 5(c) and 5(d) that with 0.33 ML-In pre-deposited, cobalt spreads out much more evenly across the copper surface than without indium [Figs. 5(a) and 5(b)], so that typical surface regions develop terraces with only about  $\pm 1$  ML variation in thickness.<sup>28</sup>

For higher indium coverages (0.8–2 ML), if an approximately closed indium layer were formed on the  $\text{Cu}_3\text{In}$  alloy, a scenario of cobalt atom diffusive motion on the surface buried by the topmost indium film cannot be excluded. This mechanism is like that described for growth of copper or cobalt under the influence of a monolayer of lead as surfactant on the Cu(111) surface.<sup>29,30</sup> However, for still higher indium coverages (approx. 2.5–3 ML) this mechanism reaches its limit, since the cobalt atoms can probably no longer reach the copper-indium boundary surface by unique exchanges of position, and cobalt clustering and island formation must take place in or on the indium film.

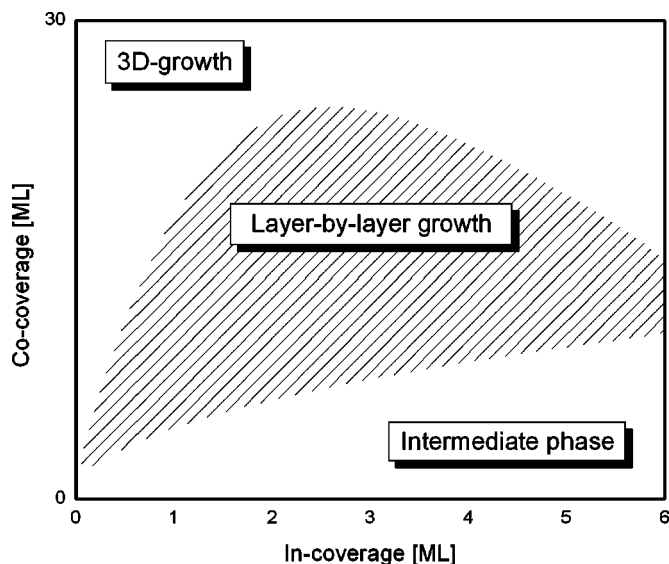


FIG. 6. Summary schematic diagram for conditions resulting in layer-by-layer growth in the presence of pre-deposited indium, 3D growth, and an intermediate phase of island growth at low cobalt coverage.

A summary schematic diagram for conditions resulting in layer-by-layer growth is shown in Fig. 6. This figure is consistent with our data but is not to be taken quantitatively because of inadequate information about sample-to-sample variation. Relatively low coverage of pre-deposited indium acts as a surfactant, facilitating layer-by-layer growth of cobalt on Cu(111) up to 12–24 ML-Co. The “layer-by-layer growth” region was established by the observation of MEED oscillations. After deposition of sufficient cobalt (perhaps a few tens of ML), 3D island growth was observed, as shown in the upper region of the figure. The “intermediate phase” region corresponds to an absence of MEED oscillations with nonperiodic changes of spot intensity, characteristic of an island growth mode for the deposited film. Careful work to assess sample-to-sample variation and clearly define the region of layer-by-layer growth is expected to establish the lines on this “phase” diagram quantitatively.

## V. NUCLEATION AND ISLAND GROWTH

In initial stages of cobalt deposition, i.e., in conditions of very low cobalt coverage, cobalt islands are formed, but the size and number of the islands are very different depending on whether indium is pre-deposited. Figure 7 shows the distribution of cobalt island diameters when 0.25 ML-Co has been deposited on a pure copper substrate [Fig. 7(a)] and on the  $\text{Cu}_2\text{In}$  surface alloy [about 0.33 ML-In pre-deposited; Fig. 7(b)]. Because of the small amount of cobalt deposited on these surfaces, the areas of cobalt nucleation are well defined and easy to see [Figs. 5(a) and 5(c)]. What we discover from Fig. 7 is that the mean island size is much smaller for the  $\text{Cu}_2\text{In}$  surface compared to the pure copper surface (mean diameter about 1.3 vs 2.6 nm as measured by STM, both overestimated due to STM tip size).

Because the total amount of cobalt is the same for Figs. 7(a) and 7(b), the smaller island size on the  $\text{Cu}_2\text{In}$  surface is accompanied by increased island density. On the pure copper

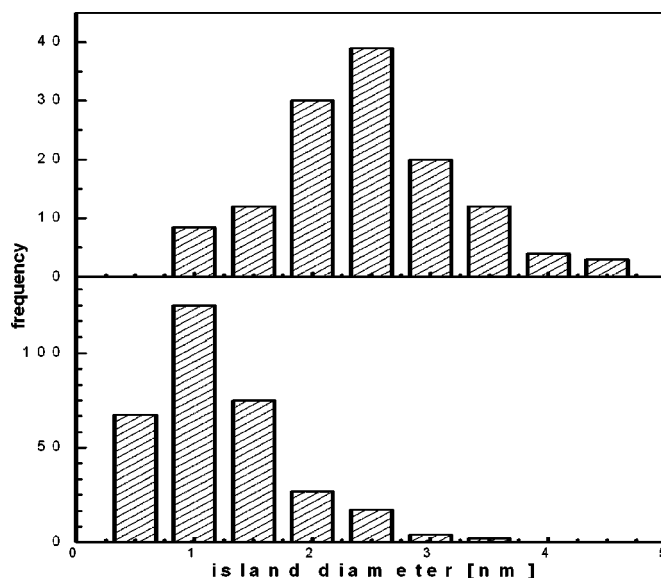


FIG. 7. Distribution of cobalt island diameters with 0.25 ML-Co deposited (a) on the pure copper substrate and (b) on the  $\text{Cu}_2\text{In}$  surface alloy (about 0.33 ML-In pre-deposited).

surface we found 380(55) islands/(100 nm)<sup>2</sup>, while on the  $\text{Cu}_2\text{In}$  surface we found 880(65) islands/(100 nm)<sup>2</sup>. There are two possible interpretations for a changed island density: decreased cobalt mobility or stress-influenced island growth. Recent Monte Carlo simulations of island growth indicate a height-growth limit for larger lattice mismatches (20% and more).<sup>31</sup> This would lead to larger island sizes for a given coverage, which is not observed in our case. Therefore, we conclude that cobalt diffusion is inhibited by the pre-deposited indium, resulting in smaller but more abundant islands. It is possible to deduce the increase of the diffusion energy barrier using Venables’s rate equations model for the kinetics.<sup>32,33</sup> Here we make the reasonable assumptions that the critical cluster size is a dimer and that the evaporation parameters and diffusivity prefactor,  $D_0$ , are the same for the two deposition surfaces. Then from the ratio of the island densities we find that the pre-deposited indium increases the activation energy for cobalt surface diffusion by about 0.06 eV. Prieto, de la Figuera, and Miranda found a surface diffusion barrier of 0.19 eV for cobalt atoms on Cu(111).<sup>27</sup> So the presence of indium increases the activation energy for cobalt surface diffusion to approximately 0.25 eV.

Finally, the increase of the surface diffusion barrier entails a decreased influence of the Ehrlich–Schwoebel (ES) barrier that inhibits atoms moving over an edge from one terrace to a lower one. (This is simply due to the fact that the step-diffusion energy barrier is the sum of the surface diffusion barrier and the ES barrier, and assuming that the effects of indium are not localized in steps.) The ES barrier is an important factor in driving 3D vs 2D growth, because with an ES barrier being relatively high compared to the surface diffusion barrier, atoms have difficulty moving over edges to extend a terrace into a smooth layer. Both smaller average island size, which increases the attempt frequency for leaving an island surface, and increased probability for a cobalt atom to step down from an island (i.e., reduced ratio of ES

barrier to surface diffusion barrier) cause greater mass transport between layers, thereby promoting 2D growth.

## VI. INDIUM SEGREGATION

The effects discussed above for small cobalt coverage will continue for higher coverage if indium atoms continue to be present on the cobalt film surface by segregation. In this case indium atoms at substitutional or terrace adatom positions continue to be responsible for decreased cobalt surface diffusion. The range of cobalt coverage for which layer-by-layer growth is observed (or inferred from MEED oscillations in this experiment) gives an indication of the cobalt film thickness for which continuing indium segregation to the surface is effective (see Fig. 6). For high enough cobalt coverages, we see that indium can no longer segregate effectively to the surface, and cobalt resumes 3D island growth.

## VII. CONCLUSIONS

We have observed a surfactant effect of pre-deposited indium that facilitates layer-by-layer growth of cobalt on Cu(111). The pre-deposited indium enters the Cu(111) surface substitutionally as  $\text{Cu}_2\text{In}$  or  $\text{Cu}_3\text{In}$ , depending on indium coverage. Cobalt atoms that are subsequently deposited exchange sites with indium atoms in the surface alloy and form well-defined layers, while indium segregates to the surface as more cobalt is deposited. This interpretation is supported by MEED, AES, and STM observations in the present work as well as a previously reported study of surface alloying of indium on Cu(111).<sup>25</sup>

The surfactant effect of indium is connected to a reduction in the cobalt surface diffusion rate (with increased energy barrier) and therefore lowered ratio of ES barrier to surface diffusion barrier. These indium-mediated changes in energy relations increase the probability for deposited cobalt atoms to move off an island and enlarge it laterally instead of growing up (3D growth).

Indium segregates to the surface by site exchange with cobalt during cobalt deposition. However, this segregation is at less than 100% efficiency, and as the cobalt thickness increases the surfactant effect diminishes until a 3D growth mode begins again.

The effect of indium on the cobalt growth mode in this system is summarized schematically in Fig. 6, showing regions of layer-by-layer growth in the presence of pre-deposited indium, 3D-growth, and an intermediate phase of island growth at low cobalt coverage.

## ACKNOWLEDGMENTS

The authors acknowledge the support of a German-Polish "Bilateral Cooperation in Science and Technology" Grant (POL-98-039) from the Bundesministerium für Bildung und Forschung and State Committee for Scientific Re-

search, as well as support from the Deutsche Forschungsgemeinschaft (SFB 513), the German-American Fulbright Commission (WEE), and the Department of Physics & Astronomy, Brigham Young University (WEE).

- <sup>1</sup>P. Grünberg, R. Schreiber, Y. Pang, M. B. Brodsky, and H. Sowers, *Phys. Rev. Lett.* **57**, 2442 (1986).
- <sup>2</sup>S. S. P. Parkin, N. More, and K. P. Roche, *Phys. Rev. Lett.* **64**, 2304 (1990).
- <sup>3</sup>S. S. P. Parkin, R. Bhadra, and K. P. Roche, *Phys. Rev. Lett.* **66**, 2152 (1991).
- <sup>4</sup>M. Baibich, J. M. Broto, A. Fert, F. Nguyen Van Dau, F. Petroff, P. Etienne, G. Creuzet, A. Friedrich, and J. Chazelas, *Phys. Rev. Lett.* **61**, 2472 (1988).
- <sup>5</sup><http://www.storage.ibm.com/ipl/oem/mrheads/mrheadtech.htm> (2001).
- <sup>6</sup>S. S. P. Parkin, Z. G. Li, and David J. Smith, *Appl. Phys. Lett.* **58**, 2710 (1991).
- <sup>7</sup>C. H. Marrows, N. Wiser, B. J. Hickey, T. P. A. Hase, and B. K. Tanner, *J. Phys.: Condens. Matter* **11**, 81 (1999).
- <sup>8</sup>S. S. P. Parkin, *IBM J. Res. Dev.* **42**, 3 (1998).
- <sup>9</sup>P. Weinberger and L. Szunyogh, *J. Phys.: Condens. Matter* **15**, S479 (2003).
- <sup>10</sup>W. F. M. Egelhoff, Jr. and T. Kief, *Phys. Rev. B* **45**, 7795 (1992).
- <sup>11</sup>S. S. P. Parkin, R. F. Marks, R. F. C. Farrow, G. R. Harp, Q. H. Lam, and R. J. Savoy, *Phys. Rev. B* **46**, 9262 (1992).
- <sup>12</sup>M. T. Johnson, R. Coehoorn, J. J. de Vries, N. W. E. McGee, J. van de Stegge, and P. J. H. Bloemen, *Phys. Rev. Lett.* **69**, 969 (1992).
- <sup>13</sup>A. Schreyer, K. Bröhl, J. F. Ankner, C. F. Majkrzak, Th. Zeidler, P. Bödeker, N. Metoki, and H. Zabel, *Phys. Rev. B* **47**, 15334 (1993).
- <sup>14</sup>B. P. Tonner, Z.-L. Han, and J. Zhang, *Phys. Rev. B* **47**, 9723 (1993).
- <sup>15</sup>J. de la Figuera, J. E. Prieto, C. Ocal, and R. Miranda, *Phys. Rev. B* **47**, 13043 (1993).
- <sup>16</sup>J. Camarero, L. Spendeler, G. Schmidt, K. Heinz, J. J. de Miguel, and R. Miranda, *Phys. Rev. Lett.* **73**, 2448 (1994).
- <sup>17</sup>D. A. Steigerwald, I. Jacob, and W. F. Egelhoff, *Surf. Sci.* **202**, 472 (1988).
- <sup>18</sup>H. A. van der Vegt, H. M. van Pinxteren, M. Lohmeier, and E. Vlieg, *Phys. Rev. Lett.* **68**, 3335 (1992).
- <sup>19</sup>J. Vrijmoeth, H. A. van der Vegt, J. A. Meyer, E. Vlieg, and R. J. Behm, *Phys. Rev. Lett.* **72**, 3843 (1994).
- <sup>20</sup>J. A. Meyer, H. A. van der Vegt, J. Vrijmoeth, E. Vlieg, and R. J. Behm, *Surf. Sci.* **355**, L375 (1996).
- <sup>21</sup>H. A. van der Vegt, M. Breeman, S. Ferrer, V. H. Etgens, X. Torrelles, P. Fajardo, and E. Vlieg, *Phys. Rev. B* **51**, 14806 (1995).
- <sup>22</sup>H. A. van der Vegt, J. Alvarez, X. Torrelles, S. Ferrer, and E. Vlieg, *Phys. Rev. B* **52**, 17443 (1995).
- <sup>23</sup>J. W. M. Frenken, R. van Gastel, S. B. van Albada, E. Somfai, and W. van Saarloos, *Appl. Phys. A: Mater. Sci. Process.* **75**, 11 (2002).
- <sup>24</sup>N. W. Alcock, *Bonding and Structure* (Horwood, New York, 1990). See [www.iumsc.indiana.edu/radii.html](http://www.iumsc.indiana.edu/radii.html).
- <sup>25</sup>H. Wider, V. Gimple, W. Evenson, G. Schatz, J. Jaworski, J. Prokop, and M. Marszałek, *J. Phys.: Condens. Matter* **15**, 1909 (2003).
- <sup>26</sup>J. de la Figuera, J. E. Prieto, C. Ocal, and R. Miranda, *Phys. Rev. B* **47**, 13043 (1993).
- <sup>27</sup>J. E. Prieto, J. de la Figuera, and R. Miranda, *Phys. Rev. B* **62**, 2126 (2000).
- <sup>28</sup>H. Wider, dissertation, University of Konstanz, 2002 (online publication at <http://www.ub.uni-konstanz.de/kops/volltexte/2002/873>).
- <sup>29</sup>J. Camarero, J. Ferrón, V. Cros, L. Gomez, A. L. Vázquez de Parga, J. M. Gallego, J. E. Prieto, J. J. de Miguel, and R. Miranda, *Phys. Rev. Lett.* **81**, 850 (1998).
- <sup>30</sup>S. Muller, J. E. Prieto, T. Kramer, Ch. Rath, L. Hammer, R. Miranda, and K. Heinz, *J. Phys.: Condens. Matter* **13**, 9897 (2001).
- <sup>31</sup>P. Nielaba, University of Konstanz, Germany (private communication), and K. P. Heue, diploma work, University of Konstanz, May 2000.
- <sup>32</sup>J. A. Venables, *Phys. Rev. B* **36**, 4153 (1987).
- <sup>33</sup>J. A. Venables, *Surf. Sci.* **299/300**, 798 (1994).